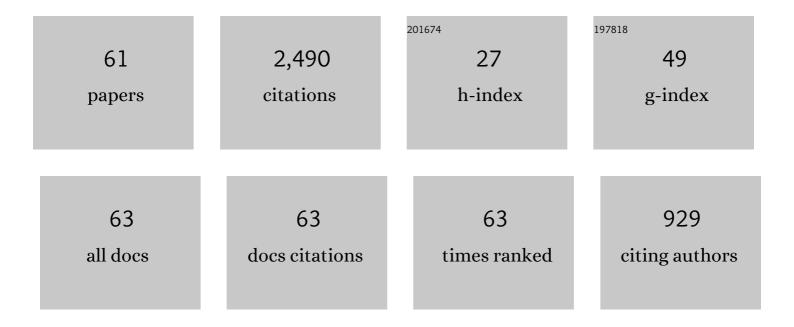
List of Publications by Year in descending order

Source: https://exaly.com/author-pdf/4268362/publications.pdf Version: 2024-02-01



7ICHEN LI

#	Article	IF	CITATIONS
1	Comparison of the real-time precise orbit determination for LEO between kinematic and reduced-dynamic modes. Measurement: Journal of the International Measurement Confederation, 2022, 187, 110224.	5.0	13
2	A satellite-based method for modeling ionospheric slant TEC from GNSS observations: algorithm and validation. GPS Solutions, 2022, 26, 1.	4.3	13
3	Real-Time Precise Orbit Determination for LEO between Kinematic and Reduced-Dynamic with Ambiguity Resolution. Aerospace, 2022, 9, 25.	2.2	11
4	Global Monitoring of Ionospheric Weather by GIRO and GNSS Data Fusion. Atmosphere, 2022, 13, 371.	2.3	20
5	The Combined Real-Time Global Ionospheric Map for Operational Ionospheric Space Weather Monitoring. , 2022, , .		1
6	Integrity investigation of global ionospheric TEC maps for high-precision positioning. Journal of Geodesy, 2021, 95, 1.	3.6	18
7	Real-time GNSS precise point positioning for low-cost smart devices. GPS Solutions, 2021, 25, 1.	4.3	54
8	Precise orbit determination of BDS-3 satellites using B1C and B2a dual-frequency measurements. GPS Solutions, 2021, 25, 1.	4.3	23
9	BeiDou Global Ionospheric delay correction Model (BDGIM): performance analysis during different levels of solar conditions. GPS Solutions, 2021, 25, 1.	4.3	18
10	Considering inter-receiver pseudorange biases for BDS-2 precise orbit determination. Measurement: Journal of the International Measurement Confederation, 2021, 177, 109251.	5.0	10
11	Sub-Auroral and Mid-Latitude GNSS ROTI Performance during Solar Cycle 24 Geomagnetic Disturbed Periods: Towards Storm's Early Sensing. Sensors, 2021, 21, 4325.	3.8	2
12	Status of CAS global ionospheric maps after the maximum of solar cycle 24. Satellite Navigation, 2021, 2, .	8.6	26
13	Lithosphere ionosphere coupling associated with three earthquakes in Pakistan from GPS and GIM TEC. Journal of Geodynamics, 2021, 147, 101860.	1.6	14
14	The cooperative IGS RT-GIMs: a reliable estimation of the global ionospheric electron content distribution inÂreal time. Earth System Science Data, 2021, 13, 4567-4582.	9.9	28
15	Inhibition of F3 Layer at Low Latitude Station Sanya During Recovery Phase of Geomagnetic Storms. Journal of Geophysical Research: Space Physics, 2021, 126, e2021JA029850.	2.4	2
16	Analysis of the short-term temporal variation of differential code bias in GNSS receiver. Measurement: Journal of the International Measurement Confederation, 2020, 153, 107448.	5.0	10
17	GPS and GLONASS observable-specific code bias estimation: comparison of solutions from the IGS and MGEX networks. Journal of Geodesy, 2020, 94, 1.	3.6	42
18	Orbital design of LEO navigation constellations and assessment of their augmentation to BDS. Advances in Space Research, 2020, 66, 1911-1923.	2.6	10

#	Article	IF	CITATIONS
19	The Impact of Different Ocean Tide Loading Models on GNSS Estimated Zenith Tropospheric Delay Using Precise Point Positioning Technique. Remote Sensing, 2020, 12, 3080.	4.0	3
20	Towards Cooperative Global Mapping of the Ionosphere: Fusion Feasibility for IGS and IRI with Global Climate VTEC Maps. Remote Sensing, 2020, 12, 3531.	4.0	25
21	A Multi-Sensor Tight Fusion Method Designed for Vehicle Navigation. Sensors, 2020, 20, 2551.	3.8	6
22	High-rate Doppler-aided cycle slip detection and repair method for low-cost single-frequency receivers. GPS Solutions, 2020, 24, 1.	4.3	30
23	IGS real-time service for global ionospheric total electron content modeling. Journal of Geodesy, 2020, 94, 1.	3.6	63
24	The Performance of Different Mapping Functions and Gradient Models in the Determination of Slant Tropospheric Delay. Remote Sensing, 2020, 12, 130.	4.0	21
25	Adaptation of the NeQuick2 model for GNSS wide-area ionospheric delay correction in China and the surrounding areas. Advances in Space Research, 2020, , .	2.6	3
26	Regional ionospheric TEC modeling based on a two-layer spherical harmonic approximation for real-time single-frequency PPP. Journal of Geodesy, 2019, 93, 1659-1671.	3.6	37
27	Quality assessment of GPS, Galileo and BeiDou-2/3 satellite broadcast group delays. Advances in Space Research, 2019, 64, 1764-1779.	2.6	20
28	Smart-RTK: Multi-GNSS kinematic positioning approach on android smart devices with Doppler-smoothed-code filter and constant acceleration model. Advances in Space Research, 2019, 64, 1662-1674.	2.6	30
29	Investigation of the performance of real-time BDS-only precise point positioning using the IGS real-time service. GPS Solutions, 2019, 23, 1.	4.3	40
30	The BeiDou global broadcast ionospheric delay correction model (BDGIM) and its preliminary performance evaluation results. Navigation, Journal of the Institute of Navigation, 2019, 66, 55-69.	2.8	122
31	Assessment of NeQuick and IRI-2016 models during different geomagnetic activities in global scale: Comparison with GPS-TEC, dSTEC, Jason-TEC and GIM. Advances in Space Research, 2019, 63, 3978-3992.	2.6	17
32	Multi-GNSS triple-frequency differential code bias (DCB) determination with precise point positioning (PPP). Journal of Geodesy, 2019, 93, 765-784.	3.6	50
33	Helmert-VCE-aided fast-WTLS approach for global ionospheric VTEC modelling using data from GNSS, satellite altimetry and radio occultation. Journal of Geodesy, 2019, 93, 877-888.	3.6	15
34	Ionospheric correction using GPS Klobuchar coefficients with an empirical night-time delay model. Advances in Space Research, 2019, 63, 886-896.	2.6	8
35	Refinement of global ionospheric coefficients for GNSS applications: Methodology and results. Advances in Space Research, 2019, 63, 343-358.	2.6	21
36	GPS, BDS and Galileo ionospheric correction models: An evaluation in range delay and position domain. Journal of Atmospheric and Solar-Terrestrial Physics, 2018, 170, 83-91.	1.6	28

#	Article	IF	CITATIONS
37	Performance of various predicted GNSS global ionospheric maps relative to GPS and JASON TEC data. GPS Solutions, 2018, 22, 1.	4.3	34
38	Consistency of seven different GNSS global ionospheric mapping techniques during one solar cycle. Journal of Geodesy, 2018, 92, 691-706.	3.6	181
39	Determination of the optimized single-layer ionospheric height for electron content measurements over China. Journal of Geodesy, 2018, 92, 169-183.	3.6	24
40	The correlation between GNSS-derived precipitable water vapor and sea surface temperature and its responses to El Niño–Southern Oscillation. Remote Sensing of Environment, 2018, 216, 1-12.	11.0	74
41	Assessment of Multiple GNSS Real-Time SSR Products from Different Analysis Centers. ISPRS International Journal of Geo-Information, 2018, 7, 85.	2.9	69
42	Validation and Assessment of Multi-GNSS Real-Time Precise Point Positioning in Simulated Kinematic Mode Using IGS Real-Time Service. Remote Sensing, 2018, 10, 337.	4.0	59
43	The First Result of Relative Positioning and Velocity Estimation Based on CAPS. Sensors, 2018, 18, 1528.	3.8	5
44	Integrity monitoring-based ambiguity validation for triple-carrier ambiguity resolution. GPS Solutions, 2017, 21, 797-810.	4.3	21
45	An examination of the Galileo NeQuick model: comparison with GPS and JASON TEC. GPS Solutions, 2017, 21, 605-615.	4.3	36
46	Estimation and analysis of Galileo differential code biases. Journal of Geodesy, 2017, 91, 279-293.	3.6	32
47	Improving the Triple-Carrier Ambiguity Resolution with a New Ionosphere-Free and Variance-Restricted Method. Remote Sensing, 2017, 9, 1108.	4.0	6
48	Smart Device-Supported BDS/GNSS Real-Time Kinematic Positioning for Sub-Meter-Level Accuracy in Urban Location-Based Services. Sensors, 2016, 16, 2201.	3.8	41
49	Influence of the timeâ€delay of correction for BDS and GPS combined realâ€ŧime differential positioning. Electronics Letters, 2016, 52, 1063-1065.	1.0	17
50	Improvement of Klobuchar model for GNSS single-frequency ionospheric delay corrections. Advances in Space Research, 2016, 57, 1555-1569.	2.6	75
51	Determination of differential code biases with multi-GNSS observations. Journal of Geodesy, 2016, 90, 209-228.	3.6	275
52	Integrity monitoring-based ratio test for GNSS integer ambiguity validation. GPS Solutions, 2016, 20, 573-585.	4.3	36
53	SHPTS: towards a new method for generating precise global ionospheric TEC map based on spherical harmonic and generalized trigonometric series functions. Journal of Geodesy, 2015, 89, 331-345.	3.6	168
54	Monitoring the ionosphere based on the Crustal Movement Observation Network of China. Geodesy and Geodynamics, 2015, 6, 73-80.	2.2	32

#	Article	IF	CITATIONS
55	New versions of the BDS/GNSS zenith tropospheric delay model IGGtrop. Journal of Geodesy, 2015, 89, 73-80.	3.6	49
56	Determination of the Differential Code Bias for Current BDS Satellites. IEEE Transactions on Geoscience and Remote Sensing, 2014, 52, 3968-3979.	6.3	49
57	Mitigation of Ionospheric Delay in GPS/BDS Single Frequency PPP: Assessment and Application. Lecture Notes in Electrical Engineering, 2014, , 477-499.	0.4	2
58	Two-step method for the determination of the differential code biases of COMPASS satellites. Journal of Geodesy, 2012, 86, 1059-1076.	3.6	146
59	Extraction of line-of-sight ionospheric observables from GPS data using precise point positioning. Science China Earth Sciences, 2012, 55, 1919-1928.	5.2	115
60	A new global zenith tropospheric delay model IGGtrop for GNSS applications. Science Bulletin, 2012, 57, 2132-2139.	1.7	78
61	Model analysis method (MAM) on the effect of the second-order ionospheric delay on GPS positioning solution. Science Bulletin, 2010, 55, 1529-1534	1.7	12